Development 134, 2195-2205 (2007) doi:10.1242/dev.004598

Progressive activation of Delta-Notch signaling from around the blastopore is required to set up a functional caudal lobe in the spider *Achaearanea tepidariorum*

Hiroki Oda[1,*], Osamu Nishimura[2], Yukako Hirao[2], Hiroshi Tarui[2], Kiyokazu Agata[3] and Yasuko Akiyama-Oda[1]

In the development of most arthropods, the caudal region of the elongating germ band (the growth zone) sequentially produces new segments. Previous work with the spider *Cupiennius salei* suggested involvement of Delta-Notch signaling in segmentation. Here, we report that, in the spider *Achaearanea tepidariorum*, the same signaling pathway exerts a different function in the presumptive caudal region before initiation of segmentation. In the developing spider embryo, the growth zone becomes morphologically apparent as a caudal lobe around the closed blastopore. We found that, preceding caudal lobe formation, transcripts of a *Delta* homolog, *At-Delta*, are expressed in evenly spaced cells in a small area covering the closing blastopore and then in a progressively wider area of the germ disc epithelium. Cells with high *At-Delta* expression are likely to be prospective mesoderm cells, which later express a *twist* homolog, *At-twist*, and individually internalize. Cells remaining at the surface begin to express a *caudal* homolog, *At-caudal*, to differentiate as caudal ectoderm. Knockdown of *At-Delta* by parental RNA interference results in overproduction of *At-twist*-expressing mesoderm cells at the expense of *At-caudal*-expressing ectoderm cells. This condition gives rise to a disorganized caudal region that fails to pattern the opisthosoma. In addition, knockdown of *Notch* and *Suppressor of Hairless* homologs produces similar phenotypes. We suggest that, in the spider, progressive activation of Delta-Notch signaling from around the blastopore leads to stochastic cell fate decisions between mesoderm and caudal ectoderm through a process of lateral inhibition to set up a functional caudal lobe.

KEY WORDS: Chelicerate, Arthropod, Delta, Notch, Growth zone, Caudal lobe, Mesoderm, Caudal ectoderm, Segmentation

INTRODUCTION

Segments consisting of ectoderm and mesoderm are characteristic of arthropod embryos. In development of most arthropods, segments in the posterior half of the future body are sequentially produced at the caudal region of the elongating germ band, which is often referred to as 'the growth zone' (Peel et al., 2005). Similar modes of segmentation are seen outside the phylum Arthropoda (e.g. in Chordata and Annelida). Whether segmentation in different bilaterian phyla occurs by common or independent origins is the subject of controversy (Davis and Patel, 1999; Peel and Akam, 2003). Recent work in spider has suggested that spider segmentation and vertebrate somitogenesis share a mechanism involving Delta and Notch, which favors a common origin model (Stollewerk et al., 2003; Schoppmeier and Damen, 2005). However, it is still not clear whether the mesodermal somites of vertebrates can be compared to arthropod segments, which consist of ectoderm and mesoderm (Patel, 2003). Understanding of developmental processes occurring before segmentation may be essential to resolve these issues.

Increasing numbers of studies in arthropods have focused on the growth zone. In the well-studied insect *Drosophila melanogaster*, all segments form almost simultaneously during early stages of embryogenesis. Thus, the *Drosophila* embryo shows no area corresponding to the growth zone at any developmental stage. Nonetheless, mechanisms regulating posterior and terminal patterning in *Drosophila* (St Johnston and Nüsslein-Volhard, 1992) have facilitated analysis of the development of the growth zone. In diverse arthropod species, the growth zone is characterized by specific expression of homologs of *Drosophila caudal* (*cad*) (Mlodzik et al., 1985; Macdonald and Struhl, 1986; Moreno and Morata, 1999; Schulz et al., 1998; Akiyama-Oda and Oda, 2003; Copf et al., 2004; Shinmyo et al., 2005). *cad* genes were shown to be essential for sequential production of the posterior segments in some species (Copf et al., 2004; Shinmyo et al., 2005). In addition to the *cad* genes, homologs of *Drosophila* maternal terminal genes, namely *torso* and *torso-like*, are required to set up or maintain a functional growth zone in the beetle *Tribolium* (Schoppmeier and Schröder, 2005). Despite these significant studies, the cellular and molecular events leading to establishment of the growth zone and the diversity of mechanisms underlying its development among arthropods are poorly understood.

Spiders, which are chelicerate arthropods, phylogenetically distant from the insects, are classical organisms that have been used for developmental study (Montgomery, 1909; Holm, 1952; Seitz, 1966; Yoshikura, 1975). Modern molecular techniques have been applied to two spider species, *Cupiennius salei* and *Achaearanea tepidariorum*. In *Achaearanea* development, the growth zone becomes morphologically apparent as a caudal lobe during stages when the germ disc is converted to a germ band (Montgomery, 1909; Yamazaki et al., 2005). These stages overlap with appearance of mesoderm cells expressing a homolog of *twist* (*twi*), *At-twi* (Yamazaki et al., 2005) and caudal ectoderm cells expressing a homolog of *cad*, *At-cad* (Akiyama-Oda and Oda, 2003). Once formed, the caudal lobe is composed of an ectodermal and a mesodermal cell layer (Montgomery, 1909). Work with *Cupiennius* has revealed dynamic expression of *Delta* among other genes at the caudal region (Damen et al., 2000; Stollewerk et al., 2003), reminiscent of the molecular oscillation

[1]JT Biohistory Research Hall, 1-1 Murasaki-cho, Takatsuki, Osaka 569-1125, Japan. [2]Genome Resource and Analysis Subunit, Center for Developmental Biology, RIKEN, 2-2-3 Minatojima-minamimachi, Chuo-ku, Kobe, Hyogo 650-0047, Japan. [3]Department of Biophysics, Graduate School of Science, Kyoto University, Kitashirakawa-Oiwake, Sakyo-ku, Kyoto 606-8502, Japan.

*Author for correspondence (e-mail: hoda@brh.co.jp)

Accepted 27 March 2007

proposed for vertebrate somitogenesis (Pourquié, 2003). RNA interference (RNAi)-mediated knockdown of several components of the Delta-Notch signaling pathway, including Delta, was shown to cause defects in the pattern of the opisthosomal segments (Stollewerk et al., 2003; Schoppmeier and Damen, 2005). However, as double-stranded RNA (dsRNA) was applied to *Cupiennius* embryos around the blastula stage by injection in to the perivitelline space (Schoppmeier and Damen, 2001), it is unclear whether target genes were silenced during stages before initiation of segmentation.

In this study, we examined the cellular and molecular events giving rise to a caudal lobe in *Achaearanea*, by taking advantage of parental RNAi, which can suppress target gene function during early stages of embryogenesis (Akiyama-Oda and Oda, 2006). We found that transcripts of a *Delta* homolog are expressed at high levels in what are likely to be prospective mesoderm cells arising from around the blastopore. Based on gene expression data and phenotypes produced by RNAi-mediated knockdown of Delta and other components of the Notch signaling pathway, we propose that Delta-Notch signaling is essential for caudal lobe formation in *Achaearanea*, preceding initiation of segmentation. Our findings reveal that formation of mesoderm and caudal ectoderm is a single event that sets up a functional caudal lobe in the *Achaearanea* embryo.

MATERIALS AND METHODS

Spiders

Laboratory stocks of the house spider *Achaearanea tepidariorum* were maintained at 25°C. Stages of *Achaearanea* development were described previously (Akiyama-Oda and Oda, 2003; Yamazaki et al., 2005).

cDNA cloning

An *Achaearanea* germ-band stage embryo cDNA library (Akiyama-Oda and Oda, 2003) was used to generate more than 9000 expressed sequence tags (ESTs), which were sequenced from the 5′ end. These include two sequences derived from a single gene closely related to *Drosophila Delta* [clone identification (ID), At_eW_009_P16 and At_eW_018_P16]. A full-length cDNA clone for this gene was isolated by re-screening the library, its nucleotide sequence was determined, and the deduced amino acid sequence of the *Delta*-related cDNA analyzed by BLASTP (hit against *Drosophila* Delta with an E-value of 1e-156), BLAST 2 sequences, ClustalW version 1.81 and PHYLIP version 3.5. Analysis confirmed that the gene is the closest relative of known *Delta* genes, and it was designated *At-Delta*. The EST collection also included *Notch* (clone ID, At_eW_027_D04) and *Suppressor of Hairless* [*Su*(*H*)] (clone ID, At_eW_016_A20) homologs, designated *At-Notch* and *At-Su*(*H*), respectively. The nucleotide sequences of a partial *At-Notch* and a partial *At-Su*(*H*) cDNA were determined. The deduced amino acid sequence of the *At-Notch* cDNA was hit against *Drosophila* Notch with an E-value of 4e-147 and that of the *At-Su*(*H*) cDNA against *Drosophila* Su(H) with an E-value of 9e-35. A short fragment of a homolog of *Drosophila hedgehog* (*hh*), designated *At-hh*, was isolated by PCR with the following primers: forward, 5′-GARGARGGNACNGGNGCNGA-3′, and reverse, 5′-ACCCARTCRAANCCNGCYTC-3′. A full-length *At-hh* cDNA clone was isolated by cDNA library screening. Phylogeny of Hh proteins including At-Hh was analyzed in a previous study (Simonnet et al., 2004). Sequences are available from GenBank under the accession numbers: *At-Delta*, AB287420; *At-Notch*, AB287421; *At-Su*(*H*), AB287422; and *At-hh*, AB125742.

Antibodies

A DNA fragment encoding the carboxyl-terminal 182 amino acids of *Achaearanea* Forkhead (At-Fkh) (Akiyama-Oda and Oda, 2003) was amplified by PCR and inserted between the *Eco*RI and *Sal*I sites of pET-28a(+) vector (Novagen, Madison, WI). Expression of the fusion protein was induced in BL21 (DE3) cells, and cell lysates were fractionated by SDS-PAGE and electroeluted from the gel. Purified protein was employed as an antigen to immunize two guinea pigs. As antiserum from one of the two animals specifically reacted to bacterially expressed At-Fkh fused to maltose-binding protein (see Fig. S1 in the supplementary material) and showed nuclear staining consistent with the expression patterns of *At-fkh* transcripts previously reported (Akiyama-Oda and Oda, 2003; Akiyama-Oda and Oda, 2006), it was used for experiments. A commercially available rabbit anti-β-catenin antiserum (C2206, Sigma-Aldrich, St Louis, MO) was used.

Staining of embryos

For immunostaining, embryos were fixed as described (Oda et al., 2005). Anti-At-Fkh and anti-β-catenin antisera were diluted 1:1000. Donkey anti-guinea pig IgG labeled with Cy3 (Chemicon, Temecula, CA) and donkey anti-rabbit IgG labeled with Cy5 (Chemicon) were used as secondary antibodies diluted 1:200. Samples were counterstained with 1 U/ml phalloidin-fluorescein (Molecular Probes, Eugene, OR) and 0.5 mg/ml DAPI (Sigma). Stained samples were examined with an Olympus IX71 microscope equipped with a cooled CCD camera (CoolSNAP HQ, Roper Scientific, Tucson, AZ) controlled by MetaMorph version 6.1 (Universal Imaging, Downington, PA).

Single- and dual-color whole-mount in situ hybridizations were performed as described (Lehmann and Tautz, 1994; Akiyama-Oda and Oda, 2006), followed by DAPI staining. All stained samples except for those shown in Fig. 1L,L′ were flat-mounted after removal of excess yolk. Embryos were photographed using a stereomicroscope (SZX12, Olympus) equipped with a color CCD camera (C7780-10, Hamamatsu Photonics, Hamamatsu, Japan), and an Axiophot2 (Carl Zeiss). Cell death was visualized using a TACS 2 TdT-DAB kit (Trevigen, Gaithersburg, MD).

Parental RNAi

The 1054 bp (nucleotide [nt] 136-1189) and 965 bp (nt 1406-2370) regions of *At-Delta* cDNA were used to synthesize *At-Delta*^{EB} and *At-Delta*^{HH} dsRNAs. Control dsRNA was synthesized using the entire coding region of jellyfish *green fluorescent protein* (*gfp*) gene (Quantum), *At-Notch* dsRNA with a 1190 bp region (nt 30-1219) of a partial *At-Notch* cDNA, and *At-Su*(*H*) dsRNA with a 580 bp region (nt 1-580) of a partial *At-Su*(*H*) cDNA. Synthesis and injection of dsRNA were performed as described (Akiyama-Oda and Oda, 2006). dsRNAs were used at concentrations of 1.5-2.0 μg/μl for injection. dsRNA solution (1-2 μl) was repeatedly introduced into the opisthosoma of each female at 2-3 day intervals. The injection was repeated five times for *At-Delta*^{EB}, *gfp* and *At-Su*(*H*) dsRNA, three (the individuals #7 and #8) or four (the individual #9) times for *At-Delta*^{HH} dsRNA, and six times for *At-Notch* dsRNA.

Time-lapse recording of live embryos

After dechorionation with 100% bleach, embryos were attached to glass coverslips with double-sided sticky tape and covered with halocarbon oil 700 (Sigma). Images were taken every 5 minutes with the above color CCD camera and processed in MetaMorph version 6.1, ImageJ version 1.32 and Adobe Premiere version 6.0 to produce the movie.

RESULTS

Characterization of five distinct cell types that internalize during early stages

Examination of embryos fixed at successive stages with several probes allowed us to identify five distinct cell types that were situated below the surface epithelial cell layer during the period between stages 4 and 7 (Fig. 1A). The center of the forming germ disc during stage 4 (Fig. 1B) was the site at which cells expressing transcripts and proteins of *At-fkh* internalized (Fig. 1C-F) (Akiyama-Oda and Oda, 2003). This site of cell internalization is referred to as the blastopore (Fig. 1B,D) (Montgomery, 1909). We designated *At-fkh*-positive cells situated below the central area of the germ disc epithelium as central endoderm (cEND) cells. Cumulus mesenchymal (CM) cells,

characterized by *decapentaplegic* (*dpp*) expression (Akiyama-Oda and Oda, 2003), appeared to originate as a subpopulation of cEND cells. In accordance with this, strong β-catenin concentration at specific sites of cell-cell contact was observed in the cEND cell cluster at late stage 4 (Fig. 1F, arrow) and in the migrating CM cell cluster during stage 5 (data not shown). After CM cells left the center of the germ disc, remaining cEND cells were scattered (Fig. 1H,J,J′,K,K′).

The rim of the germ disc (Fig. 1G) was another site of cell internalization. At mid stage 5, but not earlier, some cells expressing *At-fkh* transcripts were found below the germ disc epithelium close to the rim (Fig. 1I,I′). These internalized cells, which did not express *At-twi* transcripts (Fig. 1L,L′), were designated peripheral endoderm (pEND) cells. At mid- to late stage 5, some *At-fkh*-expressing cells located at the rim of the germ disc began to express *At-twi* transcripts (Fig. 1L,L′). These cells did not enter the inside until CM cells almost reached the rim of the germ disc (late stage 5). At approximately the beginning of stage 6, when the extraembryonic area begins to differentiate (Fig. 1M), an increasing number of *At-twi*-expressing cells was seen at and near the rim of the germ disc (Fig. 1N). All of these peripheral *At-twi*-positive cells except cells at the rim were located below the surface epithelium (data not shown). *At-twi*-positive cells situated below the peripheral epithelium were designated peripheral mesoderm (pMES) cells. After internalization, pMES cells appeared to migrate centripetally (Fig. 1N,T-W).

As previously described (Yamazaki et al., 2005), some cells around the center of the germ disc, which were apparently distinct from cEND cells, began to express *At-twi* transcripts starting at the beginning of stage 6 (Fig. 1N-Q,O′-Q′). These cells showed an evenly spaced distribution, although many were seen in pairs. Visualization of nuclei showed that *At-twi*-positive cells were at the surface or internalizing (Fig. 1O,O′,P,P′). *At-twi*-positive cells that situated below the central epithelium were designated central mesoderm (cMES) cells. New cMES cells continued to arise from an area adjacent to the growing *At-cad* expression domain (Fig. 1R-W). Our previous studies showed that in the formed caudal lobe, in addition to ectoderm cells, some mesoderm cells express *At-cad* transcripts and that expression of *At-twi* transcripts disappears (Akiyama-Oda and Oda, 2003; Yamazaki et al., 2005).

Molecular characterization of a *Delta* homolog in *Achaearanea*

EST analysis of *Achaearanea* germ-band-stage embryos identified a homolog of *Drosophila Delta*, designated *At-Delta*. Subsequent in situ hybridization analysis revealed that the *At-Delta* expression pattern was, in part, similar to that of *At-twi* at around stages 5 and 6 (see below).

The deduced amino acid sequence of At-Delta showed a Delta/Serrate/LAG-2 (DSL) domain and nine EGF-like repeats (Fig. 2A,B). The overall protein structure more closely resembled *Drosophila* Delta than *Drosophila* Serrate, and phylogenetic analysis using unambiguously alignable amino acids in the DSL domain and in EGF-like repeats 1-3 confirmed this observation (Fig. 2C). It also showed that At-Delta most closely resembled Cs-Delta1, one of two Delta homologs reported in another spider, *Cupiennius salei* (Fig. 2B,C) (Stollewerk, 2002).

Expression patterns of *At-Delta* transcripts

Expression patterns of *At-Delta* transcripts were examined by whole-mount in situ hybridization. From before mid-stage 4, *At-Delta* transcripts were detected in cells located near, but not at, the rim of the forming germ disc (Fig. 3A-C). No expression was detectable around the center of the germ disc at mid-stage 4 (Fig. 3A). In a late-stage 4 embryo, however, several cells located at the rim of the forming germ disc and all non-germ-disc surface cells expressed *At-Delta* (Fig. 3D). In the same embryo, some surface cells around the blastopore distinct from the cEND cells expressed *At-Delta* (Fig. 3D-F). During stage 5, the area displaying interspersed *At-Delta* expression expanded (Fig. 3G). *At-Delta*-expressing cells, many of which were seen in pairs, were located at the same level as the remaining cells in the epithelium (Fig. 3H). About a quarter of the surface cells at the central area displayed high-levels of *At-Delta* expression. Both paired and unpaired *At-Delta*-positive cells were evenly spaced.

By early stage 6, *At-Delta* expression began to fade from around the center of the germ disc (Fig. 3I). This process was followed by the appearance of *At-twi* transcripts, probably in prospective cMES cells (Fig. 3L,M). In support of this idea, cells positive for low levels of both *At-Delta* and *At-twi* were found in that area as *At-Delta* expression faded (Fig. 3M, arrows). Expression of *At-cad* was observed in the growing *At-Delta*-negative domain at mid-stage 6 but not early stage 6 (Fig. 3I,J). Changing expression patterns of *At-Delta*, *At-fkh*, *At-twi* and *At-cad* preceding caudal lobe formation are summarized schematically in Fig. 3N.

A second wave of *At-Delta* expression was observed in the nascent caudal lobe at late stage 6/early stage 7 (Fig. 3K). Similar to previous observations for *Cupiennius Delta* genes (Stollewerk et al., 2003), an increase in the number of stripes of *At-Delta* expression was observed in the developing opisthosomal region (Fig. 3O,P). In addition, one relatively broad band of *At-Delta* expression became prominent in the prosomal region during early germ band stages (Fig. 3O,P). In the limb-extending germ band (stage 9), *At-Delta* expression was observed in neural precursors (Fig. 3Q), as reported for *Cs-Delta1* (Stollewerk, 2002).

Parental RNAi against *At-Delta* results in defects in caudal lobe formation

To examine the function of *At-Delta* in early spider embryos, we used parental RNAi. Two types of dsRNA were prepared from non-overlapping regions of *At-Delta* cDNA, designated *At-Delta*^{EB} and *At-Delta*^{HH} dsRNAs (Fig. 2A). Females injected with *At-Delta*^{EB} or *At-Delta*^{HH} dsRNA, but not with control *gfp* dsRNA, produced embryos displaying morphological defects starting at early stage 6 (Fig. 4A-E; see Movie 1 in the supplementary material). In affected embryos, an unusual large invagination was formed around the center of the germ disc, resulting in abnormal thickening of cells at the emerging caudal region (Fig. 4B). For most females injected with *At-Delta*^{EB} or *At-Delta*^{HH} dsRNA, the penetrance of this 'invagination' phenotype was 100% (excluding embryos showing non-specific developmental defects) 2 to 3 weeks after the first injection (Fig. 4D,E). This condition lasted for another few weeks. Neither the frequency of egg-laying nor the quality of eggs was significantly affected.

Embryos displaying invagination phenotypes at stage 6 developed into various forms. Many formed either the correct or a reduced number of limbs, but formation of the germ band and extension of limbs were markedly delayed (see Movie 1 in the supplementary material). Phenotypes of late embryos were categorized as normal or consisting of three defective classes (classes 1 to 3; Fig. 5). Despite early defects, embryos of the normal class recovered a normal form (Fig. 5E). The class 1 phenotype showed a reduced opisthosoma with the prosoma developing rather normally (Fig. 5B). In many class 1 embryos, extension of limbs corresponding to the third and fourth walking legs was delayed. The class 2 phenotype

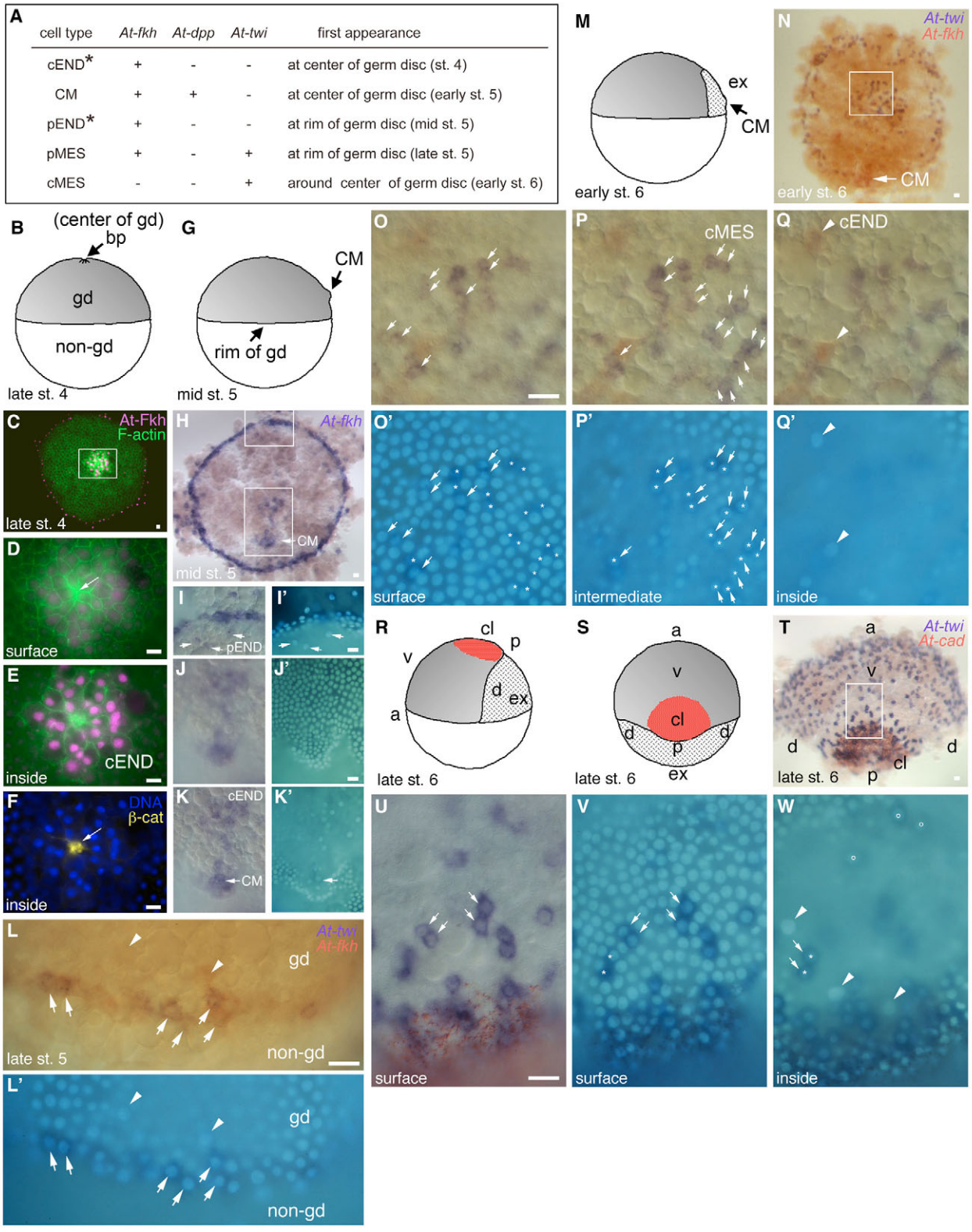

Fig. 1. See next page for legend.

displayed a loss of the entire opisthosoma, with the prosomal limbs frequently reduced in number (Fig. 5C). The class 3 phenotype showed a significant reduction of the prosoma with a disorganized germ band configuration, in addition to loss of the entire opisthosoma (Fig. 5D). Based on late phenotypes, the effect of *At-Delta*^{HH} dsRNA injection was more significant than that of *At-Delta*^{EB} dsRNA injection (Fig. 5E).

Fig. 1. Internalization of distinct cell types during early stages of *Achaearanea* embryogenesis. (**A**) Early cell types defined in terms of gene expression and site of appearance. Note that the two cell types indicated by asterisks are indistinguishable unless site of appearance is considered. (**B**) Illustration of a late stage 4 embryo. (**C-F**) A flat-mounted late stage 4 germ disc stained for F-actin (C-E, green), At-Fkh (C-E, purple), At-β-catenin (F, yellow) and DNA (F, blue). Boxed area in C is magnified in D-F (D, surface; E,F, inside). The pattern obtained by immunostaining for At-Fkh was the same as that obtained by in situ hybridization for its transcript at this stage (compare with Fig. 3D-F). Arrow in D, the closing blastopore; arrow in F, At-β-catenin concentration. cEND cells are situated just beneath the blastopore. (**G**) Illustration of a mid-stage 5 embryo. (**H-K′**) A flat-mounted mid-stage 5 germ disc stained for *At-fkh* transcripts (H-K) and DNA (I′-K′). The upper box in H corresponds to I,I′ and the lower one to J,J′,K,K′. (I,I′) pEND cells are visible near the rim of the germ disc (arrows). (J,J′,K,K′) The focal plane is adjusted to the surface layer in J and J′ and the inner layer in K and K′. cEND and CM (arrows) cells are visible. (**L**,**L′**) High magnification of the equatorial region of a late stage 5 embryo stained for *At-fkh* (L, red) and *At-twi* (L, purple) transcripts and DNA (L′). The boundary between the germ disc and non-germ disc areas is seen. Arrowheads indicate pEND cells located below the surface layer, and arrows indicate probable pMES cell precursors about to internalize. (**M**) An illustration of an early stage 6 embryo. (**N-Q′**) A flat-mounted early stage 6 germ disc stained for *At-fkh* (N-Q, red) and *At-twi* (N-Q, purple) transcripts and DNA (O′-Q′). The boxed area in N is magnified in O-Q,O′-Q′. The focal plane is adjusted to the surface layer in O and O′, an intermediate level in P and P′ and a one-cell deep level in Q and Q′. Arrows indicate cMES cell precursors, and arrowheads cEND cells. Asterisks mark the same positions in O′ and P′ to show that *At-twi*-positive cells are internalizing. (**R**,**S**) Illustrations of a late stage 6 embryo viewed from the lateral (R) or caudal (S) side. *At-cad* expression is shown in red. (**T-W**) A flat-mounted late stage 6 embryo stained for *At-twi* (T,U, purple) and *At-cad* (T,U, red) transcripts and DNA (V,W). The boxed area in T is magnified in U-W. The focal plane is adjusted to the surface layer in V and W, and a one-cell-deep level in W. Arrows indicate likely cMES cell precursors internalizing or about to internalize. Asterisks mark the same positions in U and V. Small open circles indicate pMES cells, and arrowheads cEND or pEND cells. a, anterior; bp, blastopore; cEND, central endoderm cells; cl, forming caudal lobe; CM, cumulus mesenchymal cells; cMES, central mesoderm cells; d, dorsal; ex, extraembryonic area; gd, germ disc; p, posterior; pEND, peripheral endoderm cells; pMES, peripheral mesoderm cells; v, ventral. Scale bars: 20 μm.

To confirm that defects result from suppression of *At-Delta* expression, the *At-Delta* transcripts were examined in stage 5 embryos derived from females injected with *gfp*, *At-Delta*^{EB} or *At-Delta*^{HH} dsRNA by whole-mount in situ hybridization. It was found that injection of *At-Delta*^{EB} and *At-Delta*^{HH} dsRNA but not *gfp* dsRNA disrupted the interspersed pattern of *At-Delta* expression in the germ disc (Fig. 6A,C,E) and resulted instead in a smeared pattern. High magnification of central cells of the affected germ discs revealed that there were fewer *At-Delta* transcripts in the cytoplasm, whereas most, if not all, nuclei displayed two dots of *At-Delta* transcripts possibly related to homologous chromosomes (Fig. 6B,D,F). This observation implies that *At-Delta* transcription is active, but *At-Delta* transcripts are not stable in the cytoplasm. Combined with the fact that the two dsRNAs yielded similar phenotypes, we conclude that defects seen following injection of *At-Delta*^{EB} or *At-Delta*^{HH} dsRNA result from specific degradation of *At-Delta* transcripts. Altered distribution of *At-Delta* transcripts among central cells of the germ disc were probably due to suppressed *At-Delta* function, as discussed below. Embryos in which cytoplasmic *At-Delta* transcripts were depleted after injection of *At-Delta*^{EB} or *At-Delta*^{HH} dsRNA are hereafter referred to generally as *At-Delta* RNAi embryos and specifically as *At-Delta*^{EB} or *At-Delta*^{HH} RNAi embryos.

Mesoderm and caudal ectoderm phenotypes of *At-Delta* RNAi embryos

We further investigated the cause of caudal lobe defects in *At-Delta* RNAi embryos using molecular markers of early cell types. In *At-Delta* RNAi embryos, the *At-fkh*-expressing cEND cells, including CM cells, formed and behaved normally (Fig. 7A,B). However, the number of *At-fkh*-expressing cells at the periphery of the stage 5 germ disc was markedly reduced in *At-Delta*^{HH} RNAi embryos (Fig. 7A,B), but less so in *At-Delta*^{EB} RNAi embryos (data not shown). At stage 6, there was no significant difference in the expression of *At-fkh* between control and *At-Delta*^{EB} RNAi embryos (Fig. 7C,D). By contrast, expression patterns of *At-twi* and *At-cad* were grossly defective in *At-Delta*^{EB} RNAi embryos at late stage 6 (Fig. 7E-H). All cells participating in abnormal invagination seen in *At-Delta* RNAi embryos expressed high levels of *At-twi* (Fig. 7F). Conversely, no cells in the emerging caudal region of *At-Delta* RNAi embryos expressed significant levels of *At-cad* transcripts (Fig. 7G,H). Finally, *At-Delta* RNAi embryos at stage 6 did not show *At-twi* transcripts in the peripheral region, as did control embryos (Fig. 7E,F).

Most *At-Delta*^{EB} RNAi embryos formed a bilaterally symmetrical germ band of reduced length. Such germ bands displayed a rather normal arrangement of *At-twi*-expressing cells in most of the prosomal region, but persistently exhibited a large mass of *At-twi*-expressing cells in the caudal region (Fig. 7J). This was in contrast to the normal germ band, in which *At-twi* expression is absent from the caudal lobe (Fig. 7I) (Yamazaki et al., 2005). In addition, staining for *At-hh* showed that *At-Delta*^{EB} RNAi embryos did not generate opisthosomal segments despite the rather normal segmentation seen in the prosomal region (Fig. 7K,L). These observations accounted for the class 2 phenotype. Moreover, TUNEL staining showed that there were many dying cells in the caudal region of *At-Delta* RNAi embryos, but only a few in the caudal lobe of control embryos (Fig. 7M,N).

Parental RNAi against *Notch* and *Su(H)* homologs results in similar phenotypes

To examine whether other components of the Delta-Notch signaling pathway function in *Achaearanea* caudal lobe formation, we performed parental RNAi against *At-Notch* and *At-Su(H)*. As seen with *At-Delta* dsRNAs, injection of *At-Notch* or *At-Su(H)* dsRNA resulted in embryos displaying unusual invagination around the center of the germ disc and subsequent thickening of cells at the emerging caudal region (Fig. 8A,B). However, the penetrance of the invagination phenotype in individual egg sacs after the injection of *At-Notch* and *At-Su(H)* dsRNA was not 100% (see Fig. S2 in the supplementary material). Nonetheless, expression patterns of *At-Delta*, *At-twi* and *At-cad* transcripts were affected in both *At-Notch* and *At-Su(H)* RNAi embryos derived from egg sacs with the high penetrance of the invagination phenotype (Fig. 8C-H). In these embryos, the interspersed pattern of *At-Delta* expression around the center of the germ disc was partially or completely disrupted, although levels of *At-Delta* transcripts were higher than in *At-Delta* RNAi embryos (Fig. 8C,D). At later stages, there was an increased number of *At-twi*-expressing cells and a reduced number of *At-cad*-expressing cells at the caudal region. This phenotype was similar to that seen in *At-Delta* RNAi embryos. In addition, in *At-Notch* but not *At-Su(H)* RNAi embryos, many *At-twi*-expressing cells probably

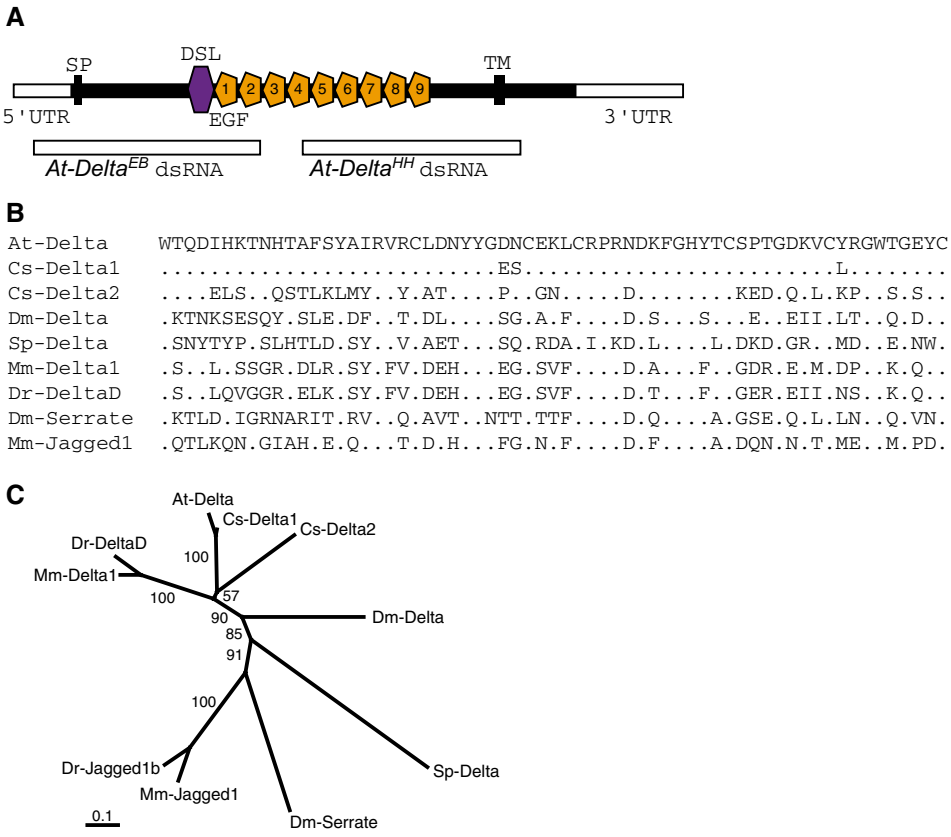

Fig. 2. Predicted amino acid sequence of *At-Delta* cDNA in *Achaearanea*. (**A**) Domain organization of At-Delta protein. Two non-overlapping regions used to synthesize *At-Delta*^{EB} and *At-Delta*^{HH} dsRNAs are shown. (**B**) Alignment of the DSL domains of Delta and other proteins. Only residues not identical to those of At-Delta are displayed. (**C**) A neighbor-joining tree constructed using 156 amino acid sites in the DSL domain and EGF repeats 1-3. The numbers at the internal branches are bootstrap values (%). Accession numbers of proteins are as follows: At-Delta (AB287420), Cs-Delta1 (CAD45190), Cs-Delta2 (CAD45191), Dm-Delta (NP_477264), Sp-Delta (NP_001027542), Mm-Delta1 (NP_031891), Dr-DeltaD (NP_571030), Dm-Serrate (CAA40148), Mm-Jagged 1 (NP_038850). At, *Achaearanea tepidariorum*; Cs, *Cupiennius salei*; Dm, *Drosophila melanogaster*; Dr, *Danio rerio*; DSL, Delta/Serrate/LAG-2 domain; EGF, EGF repeat; Mm, *Mus musculus*; Sp, *Strongylocentrotus purpuratus*; SP, signal peptide; TM, transmembrane domain.

corresponding to pMES cells were observed outside the caudal region (Fig. 8E,F), indicative of a difference between *At-Delta* and *At-Notch* RNAi embryos.

DISCUSSION

We have shown that formation of the caudal lobe in the spider *Achaearanea tepidariorum*, which precedes initiation of segmentation, requires three major components of the canonical Delta-Notch signaling pathway, namely, Delta, Notch and Su(H).

High levels of *Delta* transcripts are expressed in prospective mesoderm cells arising from around the blastopore

We described five distinguishable cell types that internalize during stages 4-7, namely cEND, CM, pEND, pMES and cMES cells. The first three are categorized as endoderm, and the last two as mesoderm. CM cells are regarded as a derivative of the cEND cells. Formation of the *Achaearanea* blastopore is associated with cEND cell internalization. Both mesodermal cell types express *At-twi*, a homolog of the *Drosophila* mesoderm-determining gene, suggesting that *Achaearanea* mesoderm is evolutionarily related to *Drosophila* mesoderm (Yamazaki et al., 2005). *At-twi*-expressing cMES cells appear to originate from multiple sites around the blastopore independently of cEND cells. This idea is reinforced by observation of evenly spaced cells expressing *At-Delta* in the central area of the germ disc epithelium at earlier stages (Fig. 3D-I) in combination with simultaneous detection of *At-Delta* and *At-twi* transcripts (Fig. 3L,M). It is likely that in normal development, the cells expressing *At-Delta* begin to express *At-twi* and enter the mesodermal pathway.

As is evident by time-lapse microscopy (see Movie 1 in the supplementary material), most surface cells of the germ disc do not significantly change positions during stages 4 and 5. Therefore, altering *At-Delta* expression patterns in the germ disc is not the result of cell movement but of progressive activation of *At-Delta* transcription. This process might be governed by a relay of short-range signals, by diffusion of long-range signals, or by graded activity of a maternal transcription factor.

Delta-Notch signaling is required to restrict the number of mesoderm cells

Defects seen after injection of *At-Delta*^{EB}, *At-Delta*^{HH}, *At-Notch* and *At-Su(H)* dsRNA were similar to each other, but completely different from those previously obtained with dsRNAs of two *Achaearanea* genes, *At-dpp* and *At-short gastrulation* (*At-sog*) (Akiyama-Oda and Oda, 2006). This situation suggests that the defects reveal specific developmental processes requiring canonical Delta-Notch signaling. Like *Cupiennius*, however, *Achaearanea* might have a second *Delta* gene and/or a second *Notch* gene. The possibility that such genes might have been additionally silenced in the RNAi experiments is not excluded.

Although it is a useful marker of future cMES cells, *At-Delta* does not seem to be necessary for differentiation into mesoderm or internalization. Defects in *At-Delta* RNAi embryos suggest that Delta-Notch signaling restricts the number of cMES cells, a function reminiscent of mechanisms controlling cell fate decisions in *Drosophila* early neurogenesis (Campos-Ortega, 1993). The evenly spaced but non-stereotyped arrangement of *At-Delta*-positive cells in the germ disc epithelium as well as the ratio of *At-Delta*-positive to -negative cells could be explained by lateral inhibition (Meinhardt and Gierer, 1974; Honda et al., 1990). As the lateral inhibition hypothesis would predict,

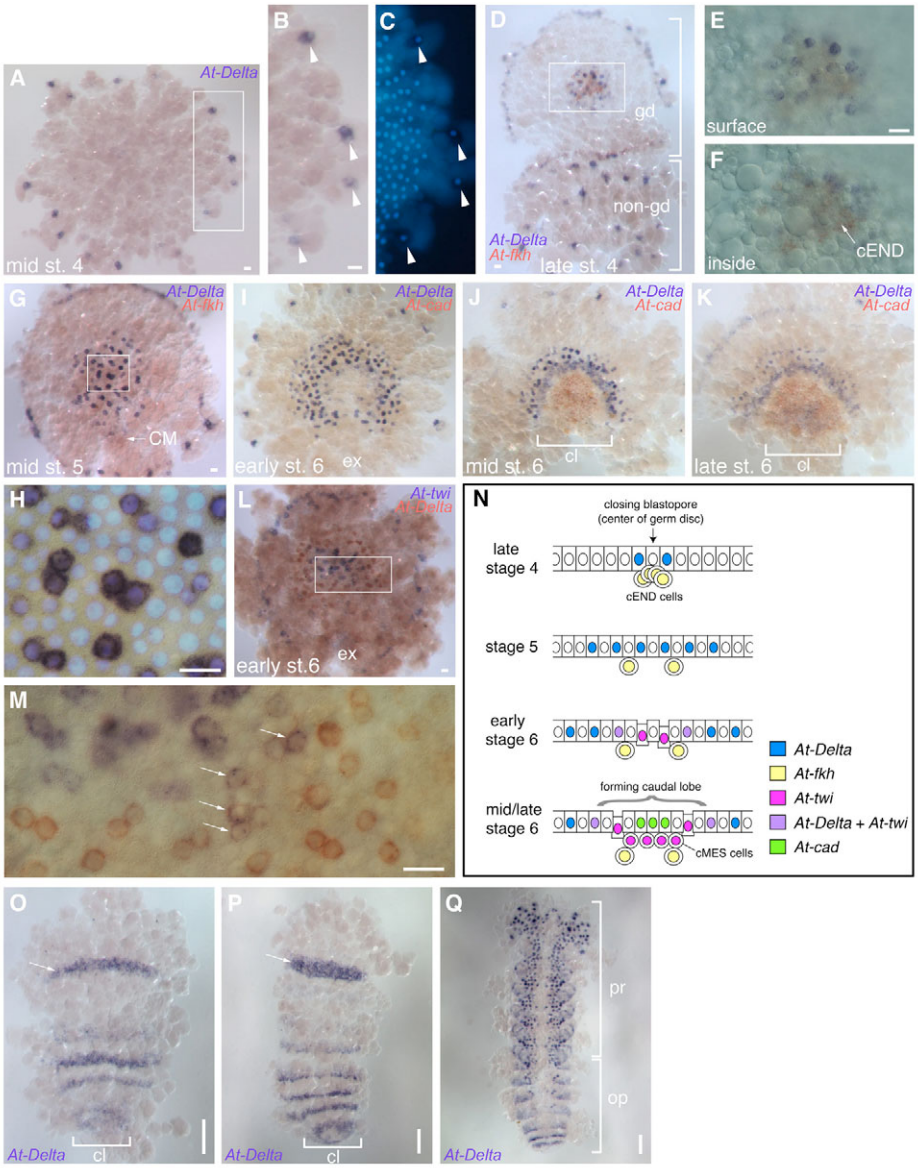

Fig. 3. Expression patterns of *At-Delta* transcripts in *Achaearanea*. (**A-C**) A flat-mounted mid-stage 4 germ disc stained for *At-Delta* transcripts (A,B) and DNA (C). The boxed area in A is magnified in B and C. Arrowheads indicate *At-Delta*-expressing cells near, but not at, the rim of the forming germ disc. (**D-F**) A flat-mounted late stage 4 embryo stained for *At-fkh* (red), *At-Delta* (purple) transcripts and DNA (not shown). Both the germ disc (gd) and non-germ disc (non-gd) areas are presented. Nuclei of non-germ disc cells show a sparse distribution. All nuclei of non-germ disc cells in D were confirmed to associate with the signals of *At-Delta* (data not shown). The boxed area in D is magnified in E (surface) and F (inside). The *At-Delta*-expressing cells are distinct from cEND cells. (**G**,**H**) A flat-mounted mid-stage 5 germ disc stained for *At-fkh* (red) and *At-Delta* (purple) transcripts and DNA. The boxed area in G is magnified in H, which is merged with DNA staining (H, light blue). Paired and unpaired *At-Delta*-positive cells are evenly spaced. (**I-K**) Flat-mounted early (I), mid- (J) and late (K) stage 6 embryos stained for *At-Delta* (purple) and *At-cad* (red) transcripts. The area displaying interspersed *At-Delta* expression expands followed by fading from the center and appearance of *At-cad* expression. *At-cad* expression is detectable from mid-stage 6. (**L**,**M**) A flat-mounted early stage 6 germ disc stained for *At-twi* (purple) and *At-Delta* (red) transcripts. The boxed area in L is magnified in M. Arrows point at cells expressing *At-twi* and *At-Delta*. (**N**) Schematic illustrations showing changing expression patterns of *At-Delta*, *At-fkh*, *At-twi* and *At-cad* transcripts up to caudal lobe formation. (**O-Q**) Stage 7 (O), stage 8 (P) and stage 9 (Q) embryos stained for *At-Delta* transcripts. Anterior is to the top. Arrows in O and P indicate a band of *At-Delta* expression in the anterior region. This anterior expression is visible in K. Note that regularly aligned spotty signals are visible in the central nervous system. cl, caudal lobe; ex, extra-embryonic area; op, opisthosoma; pr, prosoma. Scale bars: 20 μm for A-N; 100 μm for O-Q.

suppression of the inhibitory Delta signal as well as of *At-Notch* and *At-Su(H)* function abolishes interspersed expression of *At-Delta* and concomitantly causes overproduction of a single cell type (cMES cells) at the expense of other (caudal ectoderm cells) cell types (Fig. 7F,H; Fig. 8E-H). The cells that receive the At-Delta signal may be inhibited from transcribing *At-Delta* and *At-twi* in response to a different signal and entering the mesodermal pathway. The effect of blocking Delta-Notch signaling is that all the germ disc cells in the central area are allowed to transcribe *At-Delta* and *At-twi* and take the mesodermal fate.

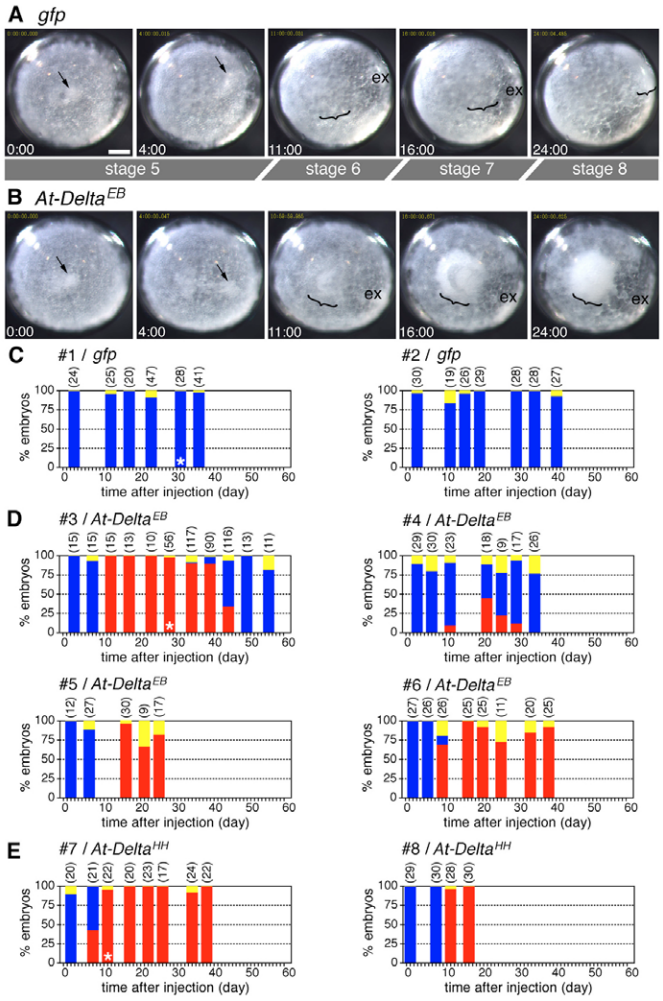

Fig. 4. Defects in caudal lobe formation following injection of *At-Delta* dsRNA. (**A**,**B**) Time-lapse recording of live embryos derived from *Achaearanea* females injected with *gfp* (A) or *At-Delta*^{EB} (B) dsRNA. The time after the start of observation (early stage 5) is shown at the bottom of each image (hour: minute). CM cells and the emerging caudal region are indicated by arrows and brackets, respectively. In B, an unusual invagination is seen at the emerging caudal region. (**C-E**) Timecourse of phenotype expression in caudal lobe after dsRNA injection. Each graph refers to one female injected with *gfp* (C), *At-Delta*^{EB} (D) or *At-Delta*^{HH} (E) dsRNA. #1-8 are identification numbers of individual females. Each vertical bar indicates relative numbers of embryos exhibiting normal (blue), invagination (red), and non-specific (yellow) phenotypes in each egg sac. The number at the top of each bar indicates the total number of embryos examined. Not all egg sacs produced by the females are presented. Unfertilized eggs and embryos that did not form morphologically normal germ disc were excluded from analysis. 'Non-specific' phenotypes, which are often observed even in embryos derived from untreated females, include shrinking, thickening and destruction of germ disc. The asterisks in #1/*gfp*, #3/*At-Delta*^{EB} and #7/*At-Delta*^{HH} indicate egg sacs used for Fig. 5. Scale bar: 100 μm. ex, extra-embryonic area.

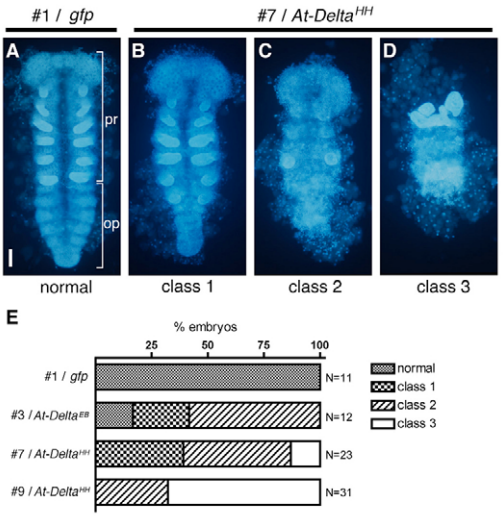

Fig. 5. Abnormal germ-band configurations following injection of *At-Delta* dsRNA in *Achaearanea*. (**A-D**) Flat preparations of a normal limb-extending embryo derived from #1/*gfp* (A) and embryos from #7/*At-Delta*^{HH} (B-D). All embryos in B-D were fixed at the same time. Prosomal regions of germ bands in A and B display similar shapes. Phenotypes of germ bands resulting from injection of *At-Delta* dsRNA are categorized as class 1 (B), class 2 (C) and class 3 (D). See text for details. (**E**) Relative numbers of embryos exhibiting normal, class 1, class 2 and class 3 phenotypes in the egg sacs indicated (see also Fig. 4). Data indicated by #9/*At-Delta*^{HH} were collected from an egg sac produced by another female 30 days after the first *At-Delta*^{HH} dsRNA injection. Scale bar: 100 μm.

Although Delta-Notch signaling does not function in specification of the primary mesoderm in *Drosophila*, its activity is required for specification of the mesectoderm (or the ventral midline cells) flanking the mesoderm in the cellularizing embryo (Menne and Klämbt, 1994; Martín-Bermudo et al., 1995; Morel and Schweisguth, 2000; Bardin and Schweisguth, 2006; De Renzis et al., 2006). Thus, in both *Drosophila* and *Achaearanea*, emerging mesoderm cells influence the fate of neighboring cells via Delta-Notch signaling. It is tempting to speculate that *Drosophila* mesectoderm specification and *Achaearanea* caudal ectoderm specification share an evolutionary link. This hypothesis would require that drastic changes in the mechanisms of ventral and caudal patterning occurred after divergence of the lineages leading to *Drosophila* and *Achaearanea* (Akiyama-Oda and Oda, 2006).

By analogy with the evolutionarily conserved mechanism of *Drosophila* and vertebrate neurogenesis (Campos-Ortega, 1993; Henrique et al., 1995), in which the proneural genes promote Delta expression to confer neural competence (Campuzano and Modolell, 1992; Kunisch et al., 1994), a mesoderm-promoting gene(s) might exist upstream of *At-Delta*. Interestingly, in the pre-involuted mesoderm of the *Xenopus* gastrula, the muscle-determining factor MyoD has been identified as a direct positive regulator of Delta-1 expression (Wittenberger et al., 1999). Another example comes from studies of sea urchin embryos, in which a double repressor system involving pmar1 activates *Delta* transcription (Oliveri et al., 2002; Revilla-i-Domingo et al., 2004), which is necessary for secondary mesoderm cell specification (Sweet et al., 2002). Moreover, in the stem cell zone of the chick embryo spinal cord, FGF signaling functions to induce Delta1 expression (Akai et al., 2005). Future studies of spider embryos should identify a gene(s) activating *At-Delta* transcription around the blastopore.

In the early *Drosophila* embryo, the highest nuclear concentrations of the maternal transcription factor Dorsal directly activate zygotic transcription of the mesoderm-determining gene *twi* (Jiang et al., 1991). Characterization of differences in *Drosophila* and *Achaearanea* gene cascades leading to activation of *twi* transcription should also be the focus of future studies.

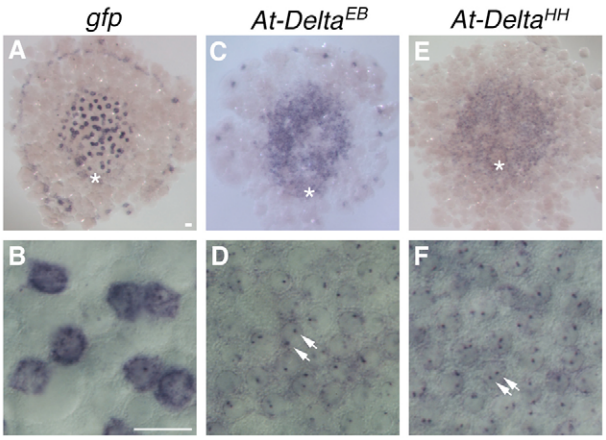

Fig. 6. Expression of *At-Delta* is affected after injection of *At-Delta* dsRNA in *Achaearanea*. Expression of *At-Delta* transcripts in germ discs derived from females injected with *gfp* (**A**,**B**), *At-Delta*^{EB} (**C**,**D**) or *At-Delta*^{HH} (**E**,**F**) dsRNA. A smear, not interspersed, pattern of *At-Delta* expression is seen in C and E. Central areas of germ discs in A,C and E are magnified in B,D and F, respectively. Arrows point at paired dots of nuclear signals implying that the transcription is active. Asterisks indicate the position of cumulus. Scale bars: 20 μm.

Delta-Notch signaling is required to induce the caudal ectoderm

Our results show that Delta-Notch signaling is essential to induce and specify caudal ectoderm in *Achaearanea* embryos. Caudal ectoderm is characterized by *At-cad* expression. Loss of the entire opisthosoma in embryos showing potent *At-Delta* RNAi phenotypes may be attributed to almost complete failure to generate *At-cad*-expressing caudal ectoderm cells. Our data indicate that zygotic *At-cad* transcription is activated downstream of Delta-Notch signaling. However, as there is a significant time lag (more than 10 hours) between initial elevation of *At-Delta* transcription around the closing blastopore (late stage 4) and the onset of *At-cad* transcription at the forming caudal lobe (mid stage 6), it is unlikely that *At-cad* is a direct target of Delta-Notch signaling.

In severe *At-Delta* RNAi embryos, overproduced mesoderm cells do not form repeating structures. Despite the fact that some mesoderm cells in the normally formed caudal lobe express *At-cad* (Akiyama-Oda and Oda, 2003), *At-cad* transcripts were not expressed in overproduced mesoderm cells in *At-Delta* RNAi embryos. Although *At-twi* transcripts disappear in the normally formed caudal lobe (Fig. 7I) (Yamazaki et al., 2005), overproduced mesoderm cells continued to express *At-twi* in the *At-Delta* RNAi embryos (Fig. 7J). These data suggest that regulation of gene expression in caudal lobe mesoderm may be influenced by ectoderm.

Opisthosomal defects that we observed in *At-Delta* RNAi embryos are due to failure in caudal lobe formation rather than in segmentation. Curiously, in previous *Cupiennius* studies, investigators described morphological abnormalities of the caudal region in embryos injected with dsRNAs targeted to components of the Delta-Notch signaling pathway (Stollewerk et al., 2003; Schoppmeier and Damen, 2005). The cause of those segmentation defects is unclear, and, in addition, mesoderm development has been poorly described in *Cupiennius*. Potential discrepancies between the *Cupiennius* and *Achaearanea* studies may arise from developmental variations between the species and/or from different experimental approaches to performing RNAi (Schoppmeier and Damen, 2001; Akiyama-Oda and Oda, 2006).

Mesoderm and caudal ectoderm formation are a single event required to establish a normal caudal lobe

We propose that in the process of caudal lobe formation, At-Delta functions both to prevent cells from adopting the mesoderm fate and to specify caudal ectoderm fate. These two outcomes may

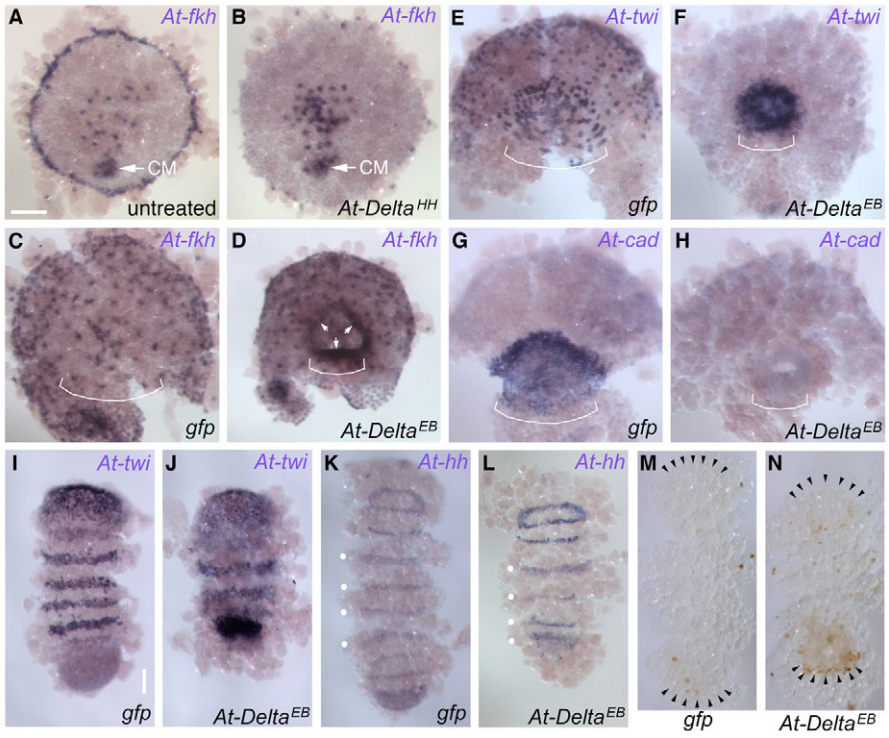

Fig. 7. Altered gene expression in *At-Delta* RNAi embryos in *Achaearanea*. (**A-D**) Staining for *At-fkh* transcripts. (A,B) Untreated (A) and *At-Delta*^{HH} RNAi (B) germ discs at stage 5. CM cells are indicated by arrows. The number of *At-fkh*-expressing cells at the periphery of the *At-Delta*^{HH} RNAi germ disc is largely reduced. (C,D) *gfp* (C) and *At-Delta*^{EB} (D) RNAi germ discs at stage 6. *At-fkh*-expressing cells are seen in central and peripheral areas. The dark areas indicated by arrows in D are due to thick folds of the cell sheet, not significant signals. (**E-H**) *gfp* (E,G) and *At-Delta*^{EB} (F,H) RNAi embryos at late stage 6 stained for *At-twi* (E,F) or *At-cad* (G,H) transcripts. The emerging caudal region is indicated by brackets in C-H. In *At-Delta*^{EB} RNAi embryos, *At-twi*-expressing cells were overproduced at the expense of *At-cad*-expressing cells. (**I-N**) *gfp* (I,K,M) and *At-Delta*^{EB} (J,L,N) RNAi embryos at early germ band stage (stage 8) stained for *At-twi* (I,J) or *At-hh* (K,L) transcripts, or for cell death (M,N). The caudal region of *At-Delta*^{EB} RNAi germ bands was grossly affected. In K and L, dots indicate segments corresponding to the four pairs of walking legs. In M and N, arrowheads indicate the anterior and posterior ends of the germ band. Anterior is to the top in C-N. Scale bars: 100 μm.

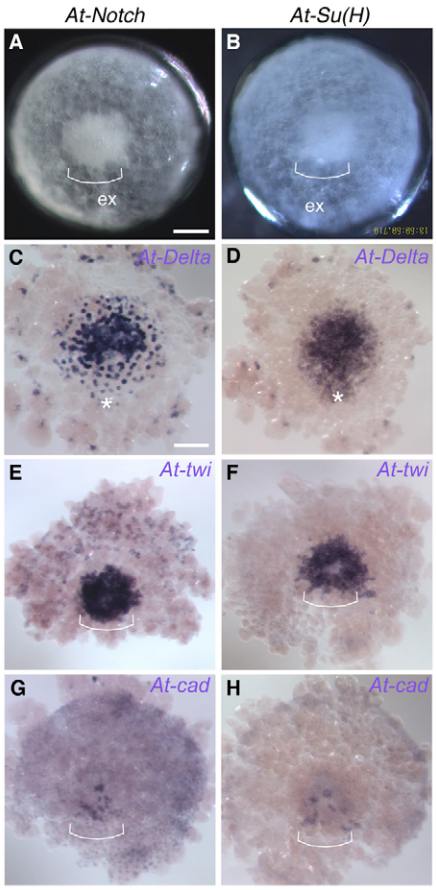

Fig. 8. Phenotypes of *At-Notch* and *At-Su(H)* RNAi embryos are similar to those of *At-Delta* RNAi embryos. (**A**,**C**,**E**,**G**) *At-Notch* RNAi embryos. (**B**,**D**,**F**,**H**) *At-Su(H)* RNAi embryos. (A,B) Live embryos at late stage 6. At the central area of each germ disc, an invagination such as seen in *At-Delta* RNAi embryos is formed (brackets). (C,D) Stage 5 germ discs stained for *At-Delta* transcripts; compare with Fig. 6A,C,E. The evenly spaced pattern of central *At-Delta* expression was partially disrupted in C, and almost completely in D. Asterisks indicate the position of cumulus. (E-H) Embryos at late stage 6 stained for *At-twi* (E,F) or *At-cad* (G,H) transcripts; compare with Fig. 7E-H. The emerging caudal region of each embryo is indicated by brackets. In E, but not in F, *At-twi*-expressing cells are seen at the peripheral areas. In G and H, only small patches of *At-cad* expression are visible. ex, extra-embryonic area. Scale bars: 100 μm.

represent interdependent outputs of Notch-mediated genetic circuits that amplify small differences between initially equivalent neighboring cells (Artavanis-Tsakonas et al., 1999). Therefore, mesoderm and caudal ectoderm formation in *Achaearanea* are not independent events but a single one achieved by Delta-Notch signaling progressively activated in the germ disc epithelium from around the blastopore. Previous work on Delta-Notch signaling in spider revived the hypothesis that arthropod segmentation and vertebrate somitogenesis have a common origin (Stollewerk et al., 2003; Tautz, 2004; Patel, 2003). However, an unanswered question is how formation of mesodermal somites in vertebrates is related to arthropod segments consisting of ectoderm and mesoderm. Our finding that mesoderm and caudal ectoderm form as a single event in spider embryos may be relevant to this issue.

Roles for *At-Delta* in other processes of *Achaearanea* development

At-Delta expression was also observed at the rim and outside of the germ disc, and *At-Delta* RNAi phenotypes potentially related to this expression include reduction of *At-fkh*-expressing cells at the rim of the germ disc at stage 5 (Fig. 7A,B), absence of *At-twi* expression outside the emerging caudal region at stage 6 (Fig. 7E,F), and delayed or defective development of the prosomal region (Figs 4, 5). Further analysis of *At-Delta* function in prosomal development is needed.

Evolution of early patterning in arthropods

In *Drosophila* embryos, cascades of maternal and zygotic transcription factors make a major contribution to anterior, posterior, terminal and dorsoventral patterning, into which germ-layer specification is integrated. These patterning systems are achieved in a syncytial environment. Similar aspects of early patterning have been reported in another insect, *Tribolium* (Sommer and Tautz, 1994; Chen et al., 2000). By contrast, our previous and present studies with the spider *Achaearanea* highlight the importance of cell-cell communication mediated by Dpp and Sog in dorsoventral patterning (Akiyama-Oda and Oda, 2006) and by Delta-Notch signaling in mesoderm and caudal specification. The necessity for cell-cell communication in early spider embryos may be due to early completion of cellularization (Kondo, 1969; Suzuki and Kondo, 1995). Based on *Achaearanea* studies, the blastopore region is particularly important, because cells producing Dpp signals originate from that region and progressive activation of Delta-Notch signaling starts there. Possibly, localized sources of intercellular signals, rather than gradients of maternal transcription factors, play central roles in early patterning in spider. Further studies with *Achaearanea* should contribute to a better understanding of the diversity of arthropod development and its ancestral mode.

We thank A. Noda for technical assistance and other members of JT Biohistory Research Hall for discussion and support.

Supplementary material

Supplementary material for this article is available at
http://dev.biologists.org/cgi/content/full/134/12/2195/DC1

References

Akai, J., Halley, P. A. and Storey, K. G. (2005). FGF-dependent Notch signaling maintains the spinal cord stem zone. *Genes Dev.* **19**, 2877-2887.
Akiyama-Oda, Y. and Oda, H. (2003). Early patterning of the spider embryo: a cluster of mesenchymal cells at the cumulus produces Dpp signals received by germ disc epithelial cells. *Development* **130**, 1735-1747.
Akiyama-Oda, Y. and Oda, H. (2006). Axis specification in the spider embryo: *dpp* is required for radial-to-axial symmetry transformation and *sog* for ventral patterning. *Development* **133**, 2347-2357.
Artavanis-Tsakonas, S., Rand, M. D. and Lake, R. J. (1999). Notch signaling: cell fate control and signal integration in development. *Science* **284**, 770-776.
Bardin, A. J. and Schweisguth, F. (2006). Bearded family members inhibit Neuralized-mediated endocytosis and signaling activity of Delta in *Drosophila*. *Dev. Cell* **10**, 245-255.
Campos-Ortega, J. A. (1993). Early neurogenesis in *Drosophila melanogaster*. In *The Development of Drosophila melanogaster* (ed. M. Bate and A. Martinez-Arias), pp. 1091-1129. New York: Cold Spring Harbor Laboratory Press.
Campuzano, S. and Modolell, J. (1992). Patterning of the *Drosophila* nervous system: the *achaete-scute* gene complex. *Trends Genet.* **8**, 202-208.
Chen, G., Handel, K. and Roth, S. (2000). The maternal NF-kappaB/Dorsal gradient of *Tribolium castaneum*: dynamics of early dorsoventral patterning in a short-germ beetle. *Development* **127**, 5145-5156.
Copf, T., Schröder, R. and Averof, M. (2004). Ancestral role of caudal genes in axis elongation and segmentation. *Proc. Natl. Acad. Sci. USA* **101**, 17711-17715.
Damen, W. G., Weller, M. and Tautz, D. (2000). Expression patterns of *hairy*, *even-skipped*, and *runt* in the spider *Cupiennius salei* imply that these genes were segmentation genes in a basal arthropod. *Proc. Natl. Acad. Sci. USA* **97**, 4515-4519.
Davis, G. K. and Patel, N. H. (1999). The origin and evolution of segmentation. *Trends Cell Biol.* **9**, M68-M72.

De Renzis, S., Yu, J., Zinzen, R. and Wieschaus, E. (2006). Dorsal-ventral pattern of Delta trafficking is established by a Snail-Tom-Neuralized pathway. *Dev. Cell* **10**, 257-264.
Henrique, D., Adam, J., Myat, A., Chitnis, A., Lewis, J. and Ish-Horowicz, D. (1995). Expression of a Delta homologue in prospective neurons in the chick. *Nature* **375**, 787-790.
Holm, Å. (1952). Experimentelle Untersuchungen über die Entwicklung und Entwicklungsphysiologie des Spinnenembryos. *Zool. Bidrag Uppsala* **29**, 293-424.
Honda, H., Tanemura, M. and Yoshida, A. (1990). Estimation of neuroblast numbers in insect neurogenesis using the lateral inhibition hypothesis of cell differentiation. *Development* **110**, 1349-1352.
Jiang, J., Kosman, D., Ip, Y. T. and Levine, M. (1991). The *dorsal* morphogen gradient regulates the mesoderm determinant twist in early *Drosophila* embryos. *Genes Dev.* **5**, 1881-1891.
Kondo, A. (1969). The fine structure of the early spider embryos. *Sci. Rep. Tokyo Kyoiku Daigaku Sect. B* **14**, 47-67.
Kunisch, M., Haenlin, M. and Campos-Ortega, J. A. (1994). Lateral inhibition mediated by the *Drosophila* neurogenic gene *delta* is enhanced by proneural proteins. *Proc. Natl. Acad. Sci. USA* **91**, 10139-10143.
Lehmann, R. and Tautz, D. (1994). In situ hybridization to RNA. *Methods Cell Biol.* **44**, 575-598.
Macdonald, P. M. and Struhl, G. (1986). A molecular gradient in early *Drosophila* embryos and its role in specifying the body pattern. *Nature* **324**, 537-545.
Martín-Bermudo, M. D., Carmena, A. and Jiménez, F. (1995). Neurogenic genes control gene expression at the transcriptional level in early neurogenesis and in mesectoderm specification. *Development* **121**, 219-224.
Meinhardt, H. and Gierer, A. (1974). Applications of a theory of biological pattern formation based on lateral inhibition. *J. Cell Sci.* **15**, 321-346.
Menne, T. V. and Klämbt, C. (1994). The formation of commissures in the *Drosophila* CNS depends on the midline cells and on the *Notch* gene. *Development* **120**, 123-133.
Mlodzik, M., Fjose, A. and Gehring, W. J. (1985). Isolation of *caudal*, a *Drosophila* homeo box-containing gene with maternal expression, whose transcripts form a concentration gradient at the pre-blastoderm stage. *EMBO J.* **4**, 2961-2969.
Montgomery, T. H., Jr (1909). The development of *Theridium*, an Aranead, up to the stage of reversion. *J. Morphol.* **20**, 297-352.
Morel, V. and Schweisguth, F. (2000). Repression by Suppressor of Hairless and activation by Notch are required to define a single row of *single-minded* expressing cells in the *Drosophila* embryo. *Genes Dev.* **14**, 377-388.
Moreno, E. and Morata, G. (1999). *Caudal* is the Hox gene that specifies the most posterior *Drosophila* segment. *Nature* **400**, 873-877.
Oda, H., Tagawa, K. and Akiyama-Oda, Y. (2005). Diversification of epithelial adherens junctions with independent reductive changes in cadherin form: identification of potential molecular synapomorphies among bilaterians. *Evol. Dev.* **7**, 376-389.
Oliveri, P., Carrick, D. M. and Davidson, E. H. (2002). A regulatory gene network that directs micromere specification in the sea urchin embryo. *Dev. Biol.* **246**, 209-228.
Patel, N. H. (2003). The ancestry of segmentation. *Dev. Cell* **5**, 2-4.
Peel, A. and Akam, M. (2003). Evolution of segmentation: rolling back the clock. *Curr. Biol.* **13**, R708-R710.
Peel, A. D., Chipman, A. D. and Akam, M. (2005). Arthropod segmentation: beyond the *Drosophila* paradigm. *Nat. Rev. Genet.* **6**, 905-916.
Pourquié, O. (2003). The segmentation clock: converting embryonic time into spatial pattern. *Science* **301**, 328-330.
Revilla-i-Domingo, R., Minokawa, T. and Davidson, E. H. (2004). R11: a cis-regulatory node of the sea urchin embryo gene network that controls early expression of SpDelta in micromeres. *Dev. Biol.* **274**, 438-451.
Schoppmeier, M. and Damen, W. G. (2001). Double-stranded RNA interference in the spider *Cupiennius salei*: the role of Distal-less is evolutionarily conserved in arthropod appendage formation. *Dev. Genes Evol.* **211**, 76-82.
Schoppmeier, M. and Damen, W. G. (2005). *Suppressor of Hairless* and *Presenilin* phenotypes imply involvement of canonical Notch-signalling in segmentation of the spider *Cupiennius salei*. *Dev. Biol.* **280**, 211-224.
Schoppmeier, M. and Schröder, R. (2005). Maternal *torso* signaling controls body axis elongation in a short germ insect. *Curr. Biol.* **15**, 2131-2136.
Schulz, C., Schröder, R., Hausdorf, B., Wolff, C. and Tautz, D. (1998). A *caudal* homologue in the short germ band beetle *Tribolium* shows similarities to both, the *Drosophila* and the vertebrate *caudal* expression patterns. *Dev. Genes Evol.* **208**, 283-289.
Seitz, V. K.-A. (1966). Normale Entwicklung des Arachniden-Embryos *Cupiennius salei* Keyserling und seine Regulationsbefähigung nach Röntgenbestrahlungen. *Zool. Jb. Anat. Bd.* **83**, 327-447.
Shinmyo, Y., Mito, T., Matsushita, T., Sarashina, I., Miyawaki, K., Ohuchi, H. and Noji, S. (2005). *caudal* is required for gnathal and thoracic patterning and for posterior elongation in the intermediate-germband cricket *Gryllus bimaculatus*. *Mech. Dev.* **122**, 231-239.
Simonnet, F., Deutsch, J. and Queinnec, E. (2004). *hedgehog* is a segment polarity gene in a crustacean and a chelicerate. *Dev. Genes Evol.* **214**, 537-545.
Sommer, R. J. and Tautz, D. (1994). Expression patterns of *twist* and *snail* in *Tribolium* (Coleoptera) suggest a homologous formation of mesoderm in long and short germ band insects. *Dev. Genet.* **15**, 32-37.
St Johnston, D. and Nüsslein-Volhard, C. (1992). The origin of pattern and polarity in the *Drosophila* embryo. *Cell* **68**, 201-219.
Stollewerk, A. (2002). Recruitment of cell groups through Delta/Notch signalling during spider neurogenesis. *Development* **129**, 5339-5348.
Stollewerk, A., Schoppmeier, M. and Damen, W. G. (2003). Involvement of *Notch* and *Delta* genes in spider segmentation. *Nature* **423**, 863-865.
Suzuki, H. and Kondo, A. (1995). Early embryonic development, including germ-disk stage, in the Theridiid spider *Achaearanea japonica* (Bös. et Str.). *J. Morphol.* **224**, 147-157.
Sweet, H. C., Gehring, M. and Ettensohn, C. A. (2002). LvDelta is a mesoderm-inducing signal in the sea urchin embryo and can endow blastomeres with organizer-like properties. *Development* **129**, 1945-1955.
Tautz, D. (2004). Segmentation. *Dev. Cell* **7**, 301-312.
Wittenberger, T., Steinbach, O. C., Authaler, A., Kopan, R. and Rupp, R. A. (1999). MyoD stimulates *delta-1* transcription and triggers notch signaling in the *Xenopus* gastrula. *EMBO J.* **18**, 1915-1922.
Yamazaki, K., Akiyama-Oda, Y. and Oda, H. (2005). Expression patterns of a *twist*-related gene in embryos of the spider *Achaearanea tepidariorum* reveal divergent aspects of mesoderm development in the fly and spider. *Zool. Sci.* **22**, 177-185.
Yoshikura, M. (1975). Comparative embryology and phylogeny of Arachnida. *Kumamoto J. Sci. Biol.* **12**, 71-142.